Theoretical Study on the Diels−Alder Reaction between 2-Methylacrolein and Cyclopentadiene Catalyzed by a Cationic Oxazaborolidine Lewis Acid

Zongxin Pi and Shuhua Li*

School of Chemistry and Chemical Engineering, Institute of Theoretical and Computational Chemistry, Laboratory of Mesoscopic Chemistry, Nanjing University, Nanjing, 210093, People's Republic of China

Received: April 14, 2006; In Final Form: May 30, 2006

The reaction mechanism of the Diels−Alder reaction between 2-methylacrolein and cyclopentadiene catalyzed by a cationic oxazaborolidine Lewis acid has been characterized using density functional theory calculations. The solvent effect on the studied reaction is taken into account by optimizing all stationary points in CH_2Cl_2 using the polarizable-continuum model. Our calculations show that the presence of this cationic oxazaborolidine catalyst changes the molecular mechanism of the studied reaction from concerted to stepwise, and lowers the activation barrier by more than 10.0 kcal/mol. A comparison of the results obtained for four different reaction channels reveals that the studied reaction is energetically favorable to occur along the *exo*/*s*-*cis* channel, which reasonably explains the stereoselectivity of the title reaction observed in related experiments. The electronic effect of this cationic oxazaborolidine complex in catalyzing the title reaction is found to be very similar to that of the commonly used Lewis acid BF_3.

1. Introduction

It is well-known that for many Diels−Alder (DA) reactions the presence of Lewis acid catalysts not only accelerates the reaction rates but also enhances the regio- and stereoselectivities in comparison with the uncatalyzed processes.[1] Therefore, the search for more efficient Lewis acid catalysts in enantioselective DA reactions has been an active field in organic chemistry. A large amount of experimental and theoretical work has been carried out to understand the effects of the Lewis acid catalysts on the nature of the molecular mechanisms of these DA reactions. Experimentally, various Lewis acid catalysts such as boron trifluoride (BF_3) and aluminum trichloride ($AlCl_3$), metal centers, and arylboron difluorides have been explored to improve the results of enantioselective DA reactions.[1] The role of the Lewis acid catalyst was theoretically investigated by studying the related reaction with BH_3 as a model catalyst in most cases (BF_3 or $AlCl_3$ in some cases). For example, Birney and Houk[2] carried out the first ab initio study on the DA reaction between butadiene and acrolein catalyzed by BH_3. Later, the same reaction was theoretically studied by Yamabe et al.[3] and García et al.,[4] but with BF_3 (or $AlCl_3$) as the model catalyst. Recently, the BF_3-catalyzed DA reaction between furan and methyl vinyl ketone[5] and the Et_2AlCl-catalyzed reaction between isoprene and acrolein[6] were theoretically investigated by density functional theory (DFT) calculations.

In a recent experimental study, Corey and co-workers reported a new type of catalytic enantioselective DA reaction with the cationic oxazaborolidine (shown in Scheme 1) as a Lewis acid catalyst.[7] This catalyst was found to effectively catalyze DA reactions between 2-methyl- or 2-bromoacrolein and a variety of 1,3-dienes at low temperature. Excellent yields and enantioselectivities were achieved for these reactions. To the best of our knowledge, the molecular mechanism of this type of DA reaction has not been studied theoretically.

In this paper, our aim is to theoretically explore the potential energy profiles of the reaction between cyclopentadiene (Cp) and 2-methylacrolein (MA) catalyzed by this cationic oxazaborolidine complex to shed light on the mechanistic details of this reaction. Since calculations with experimental catalysts are computationally demanding, we have used simple groups (R_2 = H) to replace more bulky substituents in the experimental catalysts. Due to this simplification, this study may not fully explain the origin of high enantioselectivities observed in experiments. Nevertheless, the present study is expected to allow us to better understand the effect of the Lewis acidity on the reaction mechanism of the DA reaction. For the purpose of comparison, the reaction between Cp and MA catalyzed by the commonly used BF_3 and the uncatalyzed reaction will also be studied.

2. Computational Details

All calculations were carried out at the density functional theory level with the three-parameter hybrid exchange functional of Becke and the Lee, Yang, and Parr correlation functional (B3LYP),[8] using the Gaussian 03 program.[9]

The solvent effects were considered using a self-consistent reaction field (SCRF)[10] method, based on the polarizable-continuum model (PCM)[11] with UAHF parametrization. For both catalyzed and uncatalyzed reactions, each stationary point was fully optimized in CH_2Cl_2 using the PCM model at the B3LYP level. We have used the synchronous transit-guided quasi-Newton method (STQN) for locating transition structures. For the hydrogen atoms in the proline ring of the catalyst, which were not directly bonded to the atoms involved in the reaction, we have used the 6-31G* basis set for simplicity. For all other atoms, the 6-31G** basis set was employed. For each species, we have done a frequency calculation to verify whether it is a minimum or the transition state, and to calculate zero-point energies (ZPE), enthalpies, and free energies, in which calculated frequencies were scaled by 0.98. In the Gaussian 03 program, the solvation free energies were calculated using a reference

* To whom correspondence should be addressed. E-mail:shuhua@nju.edu.cn.

10.1021/jp062320w CCC: $33.50
Published on Web 07/01/2006

SCHEME 1

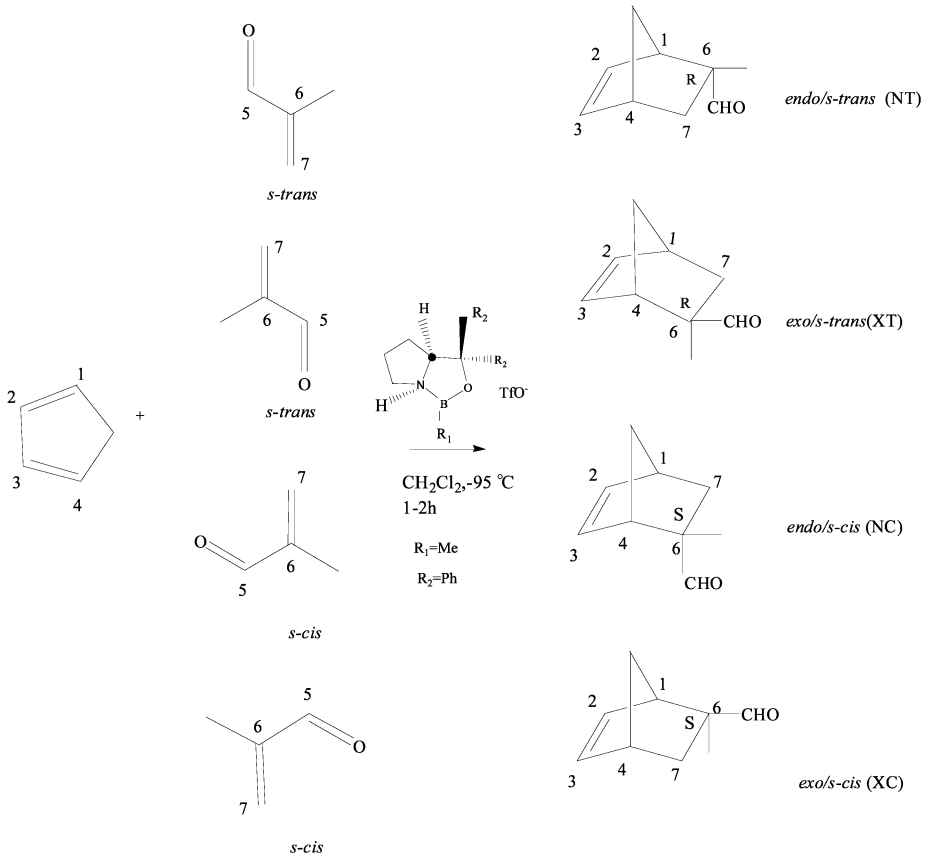

state of 1 mol/L (M), but the Gibbs free energies (*G*) for gas-phase species were determined with a reference state of 1 atm. To convert the gas-phase free energies with the reference state of 1 atm into the corresponding free energies with the reference state of 1 M, we can use the following equation:[12] $G_{gas}(1\ M) = G_{gas}(1\ atm) + RT\ \ln(14.69)$. The additional term is numerically equal to 1.60 kcal/mol at 179.0 K. Throughout this paper, the Gibbs free energies with the reference state of 1 M at 179.0 K will be used in discussing the reactivity in the solution phase.

3. Results and Discussion

The DA reaction between 2-methylacrolein (MA) and cyclopentadiene (Cp) can proceed through four different reaction pathways, depending on the approach of the cyclopentadiene with respect to the carbonyl group of the 2-methylacrolein (*exo*, *endo*) and on the conformation of the latter (*s-cis*, *s-trans*). Scheme 1 illustrates the atom numbering for the reactants and products, and four different reaction channels, which will be hereafter denoted as NT, XT, NC, and XC for simplicity. For both the uncatalyzed and catalyzed reactions, we optimized all stationary points in CH_2Cl_2 with the PCM model. A comparison of the results will allow us to shed light on the role of the catalyst in the studied DA reaction. The relative electronic energies, enthalpies, and Gibbs free energies of all the stationary points in the solution phase are given in the Supporting Information. In the following, we will first discuss the results on the uncatalyzed reaction. Then, the results on the catalyzed reaction will be presented to rationalize the role of the catalyst.

3.1. Uncatalyzed Reaction. The geometries of all stationary points are shown in Figure 1, and their relative free energies are summarized in Figure 2. Since the *s-cis* conformer of MA (abbreviated as MAC) is less stable than the *s-trans* one (MAT) by 2.66 kcal/mol in free energy, we have taken the free energy of the reactants, Cp and MAT, as the energy of zero for four reaction pathways. As shown in Figures 1 and 2, the reactions along four pathways are all concerted but asynchronous. The difference between the bond lengths of the forming bonds in the corresponding transition state is an indicator of the degree of asynchronicity. According to this indicator, one can see that **1TS**-NC and **1TS**-XC are significantly more asynchronous than **1TS**-NT and **1TS**-XT. In all four transition states (**1TS**-NC, **1TS**-XC, **1TS**-NT, **1TS**-XT), the forming bond between one carbon atom in the diene and an unsubstituted carbon in the dienophile is always significantly shorter than another forming bond involving the substituted carbon in the dienophile. In terms of frontier molecular orbital (FMO) theory, this could be ascribed to the fact that the π-orbitals between two unsubstituted carbon atoms have a better overlap and, thus, stronger bonding.[13]

The free energy barriers for the uncatalyzed reaction between MAT and Cp are 26.90 kcal/mol for **1TS**-NT and 25.36 kcal/mol for **1TS**-XT, respectively. After crossing these two transition states, the reaction would yield two cycloadducts: **2**-NT and **2**-XT, respectively. These two complexes are thermodynamically stable, which are lower in free energy by 1.05 and 1.16 kcal/mol than the reactants. By rotating the carbonyl group, **2**-NT could be easily converted into its slightly stable isomer, **4**-NT, through the transition state **3TS**-NT. Similarly, **4**-XT would be the final cycloadduct along the XT pathway, since it is more stable by 0.53 kcal/mol than **2**-XT.

The reactions between MAC and Cp would directly yield the final cycloadducts: **4**-NC and **4**-XC. Apparently, **4**-NT/**4**-NC and **4**-XT/**4**-XC are two pairs of enantiomers. Relative to the reactants Cp and MAC, the free energy barriers are 23.55 and 22.24 kcal/mol for the *endo* and *exo* pathways, respectively.

To summarize the discussions above, one can see that the activation free energies for the uncatalyzed reaction follow the

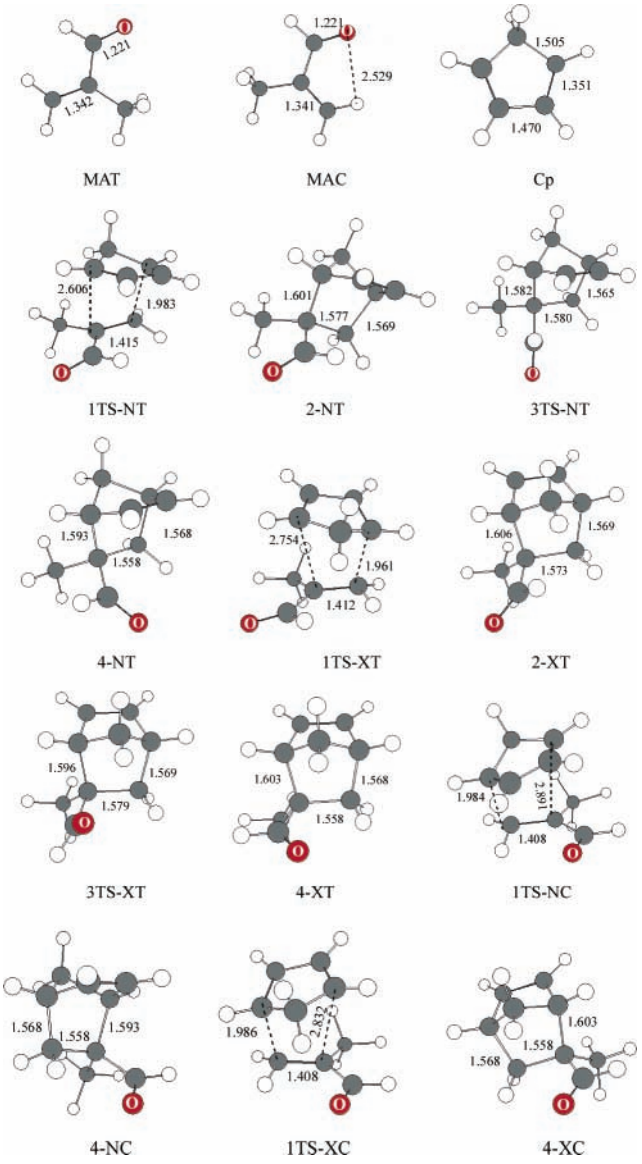

Figure 1. Optimized structures of reactants, transition states, and cycloadducts along four different reaction pathways for the uncatalyzed reaction. The bond distances are in angstroms.

order XC < NC < XT < NT. The uncatalyzed reaction is most likely to proceed through the XC channel.

3.2. Catalyzed Reaction. In the presence of the Lewis acid catalyst, the first step is the formation of the complexes between the catalyst and MA (*s-cis*, *s-trans*). Using the model catalyst **5**, we have obtained three encounter complexes, **6**, **7**, and **8**, whose structures are shown in Figure 3. One can see that MA is in a *s-trans* conformation in **6**, but in a *s-cis* conformation in **7** and **8**. In all these species, the carbonyl oxygen atom in MA is bonded to the boron atom of the catalyst **5**. In addition, in **6** and **8** a hydrogen bond between the oxygen atom of the catalyst **5** and the formyl hydrogen exists, whereas in **7** a hydrogen atom in the methylene group is involved in a similar C−H···O hydrogen bond. The Gibbs free energy changes for the formation of **6**, **7**, and **8** in CH_2Cl_2 are calculated to be −2.59, 2.94, and −1.75 kcal/mol, respectively. Thus, the encounter complex between the catalyst **5** and MA mainly exists in the form of **6** and **8**. It should be noted that if the basis set superposition error (BSSE) is taken into account by the counterpoise method,[14] we find that the complexes **6** and **8** would be thermodynamically unstable at 179.0 K. For instance, the BSSE-corrected binding

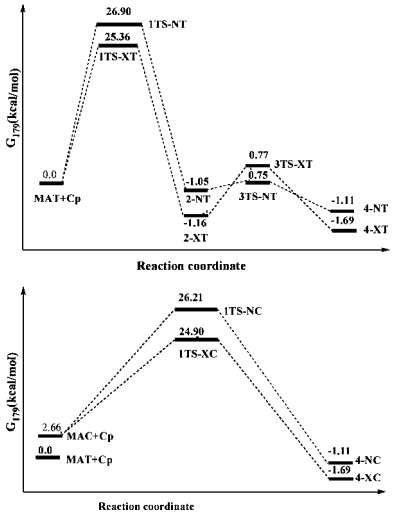

Figure 2. Free energy profiles for the uncatalyzed reaction along four different reaction pathways.

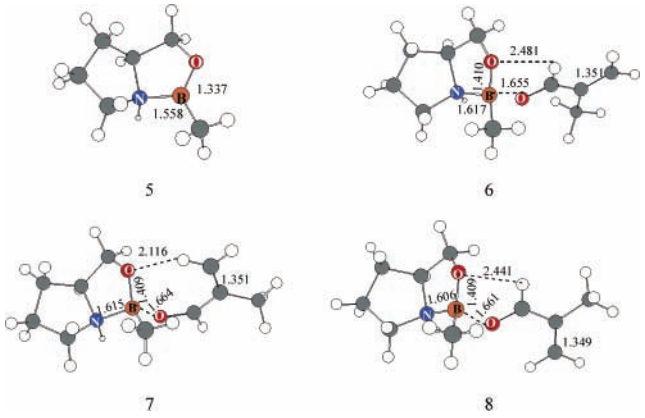

Figure 3. Optimized geometries of model catalyst **5** and catalyst−MA complexes. The bond distances are in angstroms.

free energy between MA and the catalyst **5** in **6** is 1.74 kcal/mol at 179.0 K. Thus, the BSSE is overestimated by the counterpoise method in systems **6** and **8**. This result was also observed for similar systems in a previous theoretical study.[15] As shown in Figure 3, the geometry of the catalyst is significantly changed when the catalyst is coordinated to MA. Therefore, we do not include the BSSE correction in computing the free energies of **6** and **8**. For experimental catalysts the cycloaddition between Cp and the **7**-like complex will suffer from the large steric hindrance between Cp and the phenyl groups in the catalyst. Thus, only the reaction **6** (or **8**) will be investigated in the following subsection. For each reaction, we have studied the potential energy profiles along both *endo* and *exo* channels. The optimized structures obtained for both reactions are collected in Figure 4, and their relative Gibbs free energies are shown in Figure 5.

We will first give a somewhat detailed discussion on the results for the reaction between Cp and **6**. One can see that in the presence of the catalyst the DA reaction will occur by a stepwise mechanism. Along the *endo* (or *exo*) pathway, the reaction will go through the transition state **9TS**-NT (or **9TS**-XT) to produce a zwitterionic intermediate **10**-NT (or **10**-XT). Relative to the separated reactants Cp and **6**, the activation free energies are 13.48 and 14.13 kcal/mol for **9TS**-XT and **9TS**-NT, respectively. Since only one C−C bond is formed in **10**-NT or **10**-XT, these intermediates are thermodynamically quite unstable. After passing through a very small barrier, **10**-NT will

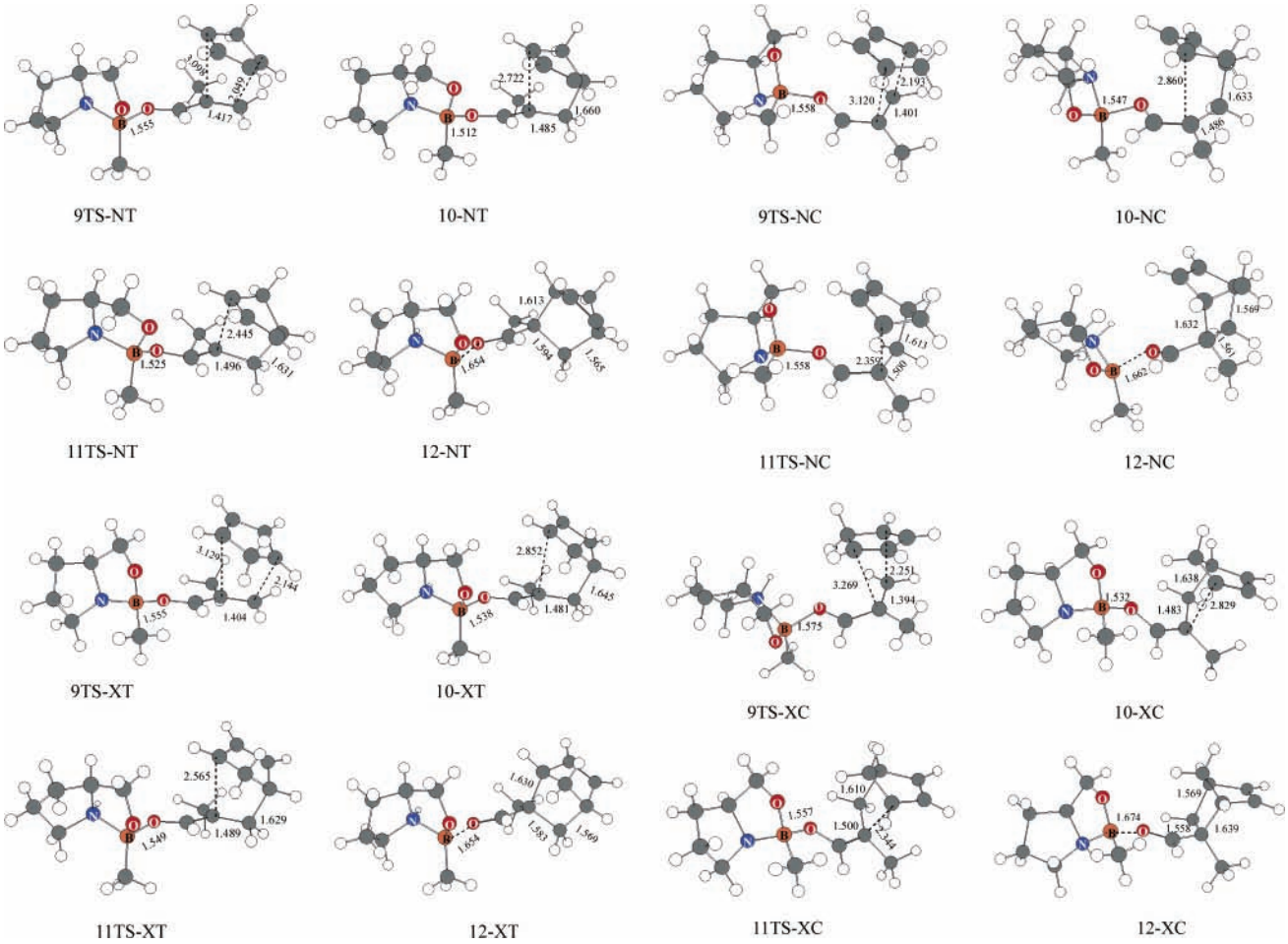

Figure 4. Optimized structures of intermediates and transition states along four different reaction pathways for the catalyzed reaction. The bond distances are in angstroms.

undergo a ring-closure process to convert into **12**-NT, which is the cycloadduct complexed with the catalyst. This step is quite exothermic (−8.14 kcal/mol), and is probably irreversible. Next, the cycloadduct **2**-NT is readily dissociated from **12**-NT, and the catalyst **5** is recovered. Finally, **2**-NT will undergo a rapid isomerization process to yield **4**-NT, which is the more stable cycloadduct, as described in the preceding subsection. Following a similar pathway, **10**-XT will convert into **4**-XT. Obviously, the rate-determining step in the catalytic cycle is the formation of the zwitterionic intermediate.

As also shown in Figure 5, the free energy profiles for the reaction between Cp and **8** share a common feature as those described above for the reaction between Cp and **6**. The rate-determining step is also the formation of the zwitterionic intermediate, with a free energy barrier of 11.60 kcal/mol for **9TS**-XC, and 13.07 kcal/mol for **9TS**-NC. A comparison of the free energy barriers of the rate-determining step in the reaction between Cp and **8**, and with those in the reaction between Cp and **6**, shows that the presence of the Lewis acid catalyst **5** does not change the order of the reactivity (XC < NC < XT < NT). As a consequence, the *exo*/*s*-*cis* (XC) channel is the most favorable channel for the DA reaction to occur. This result is in accord with the experimental observations that **4**-XC is the dominant cycloadduct.[7]

By comparing the results obtained for the catalyzed reaction with those for the uncatalyzed reaction, we can see that the main role of the catalyst is to significantly decrease the activation free energy barriers (by more than 10.0 kcal/mol). A concomitant consequence is the change of the reaction mechanism, i.e., from concerted to stepwise. Now we will give some analysis to understand how the catalyst acts in the studied DA reaction.

First, let us take a look at the geometric features of some species. For the transition states in the rate-determining step, we notice that the short forming C−C bonds in **9TS**-NT, **9TS**-XT, **9TS**-NC, and **9TS**-XC are 2.049, 2.144, 2.193, and 2.251 Å, respectively, while another forming C−C bond in these species is all around 3.100 Å, indicating that these two carbon atoms are not bonded in this step. It is interesting to compare the structures of these transition states with those of the corresponding transition states (**1TS**-NT, **1TS**-XT, **1TS**-NC, and **1TS**-XC) in the uncatalyzed reaction. A general trend is that in the concerted transition states (without the catalyst) the lengths of two forming C−C bonds are significantly shorter, especially at the substituted ends. In the zwitterionic intermediates (**10**-NT, **10**-XT, **10**-NC, and **10**-XC), the short C−C bond length is in the range of 1.63−1.66 Å, indicating that the formation of this bond is almost complete, but the long C−C bond distance of around 2.80 Å shows that these two atoms are still not bonded. By examining the $B-O_{exocyclic}$ distances in all species, we find that the bond between boron and the carbonyl oxygen ($B-O_{exocyclic}$) is noticeably shortened during the course of the cycloaddition. Once the cycloaddition reaction is complete, the $B-O_{exocyclic}$ bond length is almost restored as in the corresponding catalyst−MA encounter complex (**6** or **8**). Clearly, the electron-deficient boron plays a very important role in the cycloaddition process.

To better understand the role of the Lewis acid catalyst, it is common to make a FMO analysis. According to FMO theory,

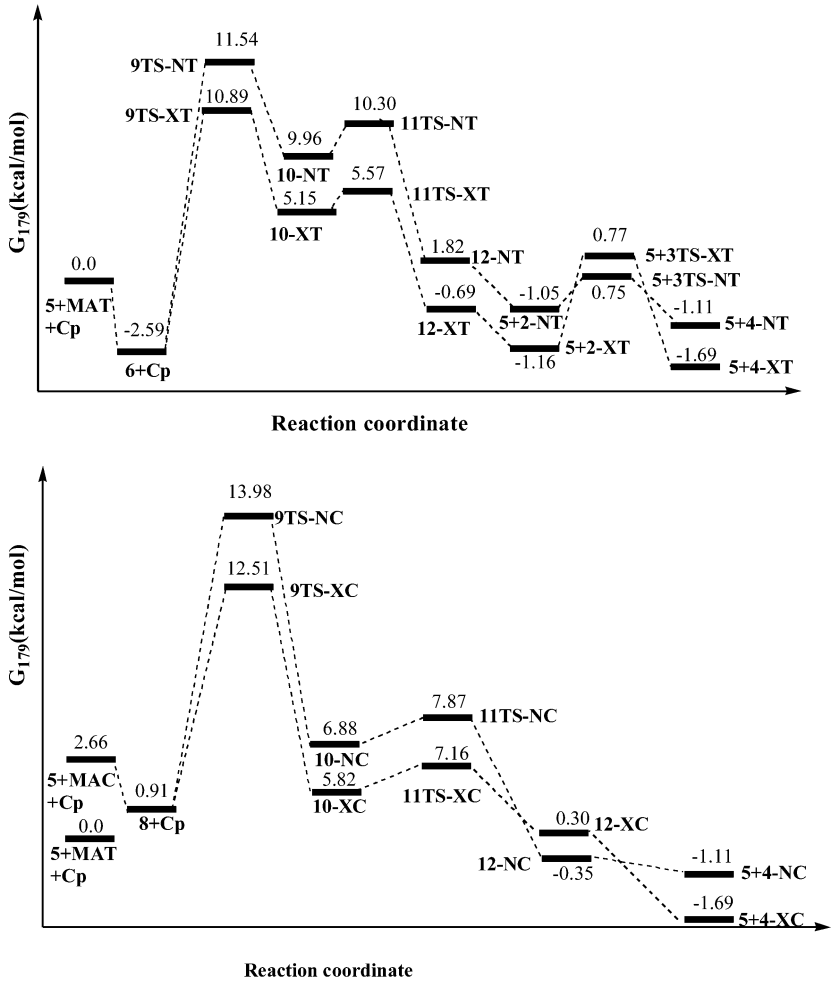

Figure 5. Free energy profiles for the catalyzed reaction along four different reaction pathways.

for a normal DA reaction a stronger highest occupied molecular orbital (HOMO)−lowest unocccupied molecular orbital (LUMO) interaction between the HOMO of the diene and the LUMO of the dienophile will lead to a relatively smaller barrier. For the studied reaction, the energies of the HOMO and LUMO of the diene (Cp), the dienophile (MAC or MAT), and the catalyst−dienophile complex (**6** or **8**) are depicted in Figure 6. One can see that the energy of the LUMO of MAT (or MAC) is lowered by about 1.82 eV (or 1.86 eV) when the Lewis acid is coordinated to MAT (or MAC). Thus, the presence of the catalyst significantly reduces the $HOMO_{diene}-LUMO_{dienophile}$ energy gap, and thus leads to a stronger $HOMO_{diene}-LUMO_{dienophile}$ interaction. This viewpoint can be further supported by the natural population analysis for the transition states in the uncatalyzed and catalyzed reactions. As listed in Table 1, the charge transfer from Cp to MA is about 0.20*e* in the transition states of the uncatalyzed reaction, but the charge transfer from Cp to the catalyst−MA complex is in the range of 0.31−0.41*e* in the transition states (of the rate-determining step) of the catalyzed reaction.

Apparently, the increase of the charge transfer is an indication of a stronger $HOMO_{diene}-LUMO_{dienophile}$ interaction induced by the electron-withdrawing catalyst.

The discussions above show clearly that the role of the catalyst **5** is to lower the energy barrier of the cycloaddition process by facilitating the delocalization of the negative charge that is transferred from the diene. It is interesting to compare the electronic behavior of the catalyst **5** with that of the commonly used Lewis acid BF_3. For this purpose, we have

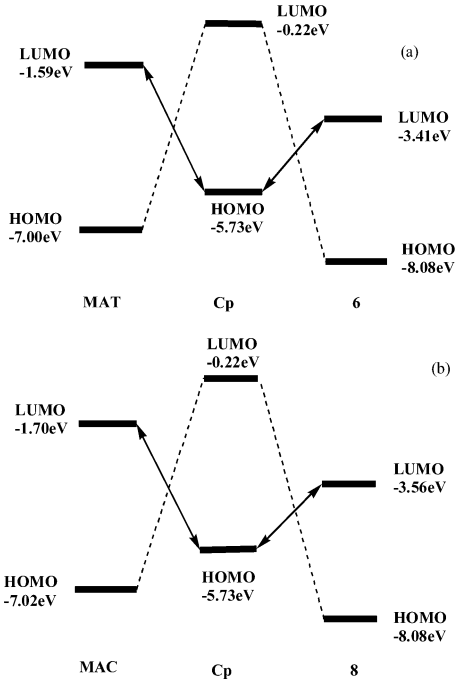

Figure 6. Energies of frontier molecular orbitals of Cp, MAT, MAC, and catalyst−MA complexes **6** and **8**.

studied the title reaction in the presence of BF_3 along the XT pathway at the B3LYP/6-31G** level. All stationary points are also optimized in CH_2Cl_2 using the PCM model. The optimized

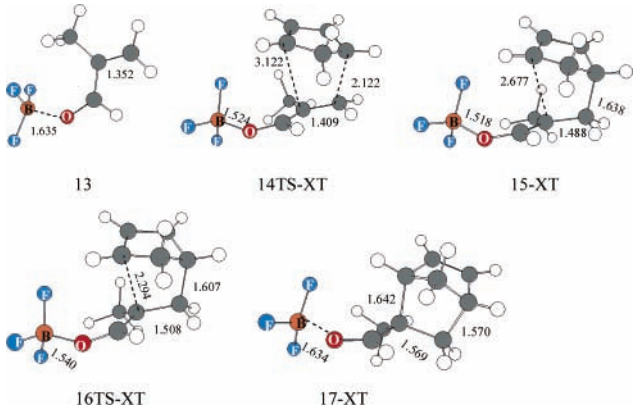

Figure 7. Optimized structures of stationary points along the XT pathway for the reaction of MAT and Cp catalyzed by BF_3. The bond distances are in angstroms.

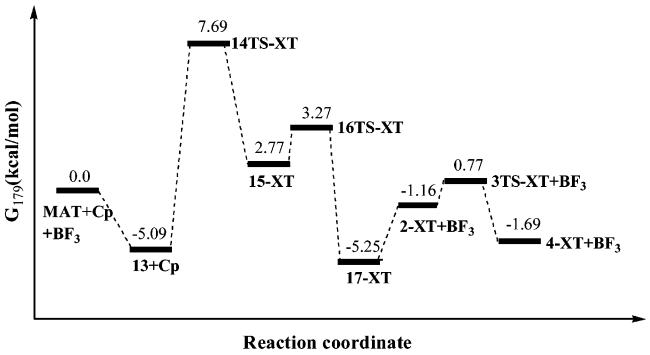

Figure 8. Free energy profiles for the reaction of MAT and Cp catalyzed by BF_3 along the XT pathway.

TABLE 1: Natural Population Analysis of the Negative Charge (in au) Transferred from Cp to MAT or MAC in the Transition States

1TS-NT	0.21	**9TS**-NT	0.41
1TS-XT	0.20	**9TS**-XT	0.36
1TS-NC	0.21	**9TS**-NC	0.36
1TS-XC	0.20	**9TS**-XC	0.31

structures are displayed in Figure 7, and the corresponding free energy profile is given in Figure 8. As one can see, a stepwise mechanism is also involved in the BF_3-catalyzed reaction. The rate-determining step, the formation of the zwitterionic intermediate (**15**-XT), is calculated to have a free energy barrier of 12.78 kcal/mol. This value is very close to the calculated barrier (13.48 kcal/mol) of the corresponding step in the presence of the catalyst **5**. In addition, we find that the charge transfer from Cp to the BF_3−MAT part in the transition state (**14TS**-XT) of the rate-determining step (0.36*e*) is almost identical to that in the corresponding transition state of the **5**-catalyzed reaction. Thus, we can see that the Lewis acidity (or the electron-withdrawing ability) of BF_3 is comparable to that of the catalyst **5**. However, by comparing the free energy profiles of the BF_3-catalyzed and **5**-catalyzed processes, we notice that in the presence of BF_3 the dissociation of the cycloadduct from the BF_3−cycloadduct complex (**17**-XT) is less thermodynamically favorable than that in the presence of the catalyst **5**.

4. Conclusions

In this work, we have carried out a theoretical study of the molecular mechanism of the Diels−Alder reaction between cyclopentadiene and 2-methylacrolein in the presence of a cationic oxazaborolidine catalyst. The solvent effect on the studied reaction is taken into account by optimizing all stationary points in CH_2Cl_2 using the PCM model. Our calculations show that in the presence of this cationic oxazaborolidine catalyst the DA reaction would take place by a stepwise mechanism. Without the catalyst, the reaction is found to occur by an asynchronous concerted mechanism. With the help of the catalyst, the rate-determining step is the nucleophilic attack of cyclopentadiene to one carbon atom of 2-methylacrolein to form the zwitterionic intermediate, which has an activation free energy barrier of about 11−14 kcal/mol, depending on the different reaction channels. The presence of the catalyst significantly lowers the activation barrier of the studied reaction (by more than 10.0 kcal/mol). A comparison of the results obtained for four different reaction channels reveals that the DA reaction is more likely to go through the *exo*/*s*-*cis* channel, which reasonably explains the stereoselectivity of the title reaction observed experimentally. Furthermore, we have compared the electronic effect of the cationic oxazaborolidine catalyst and the commonly used catalyst BF_3 in catalyzing the title reaction. These two catalysts are found to play a very similar role during the course of the DA reaction, except that BF_3 is more tightly bound to the cycloadduct.

Acknowledgment. This work was supported by the National Natural Science Foundation of China (Grants 20373022 and 20233020), the Chinese Ministry of Education (Grant NCET-04-0450), the Fok Ying Tong Education Foundation (Grant 91014), and the National Basic Research Program of China (Grant 2004CB719901).

Supporting Information Available: Total electronic energies,enthalpies, Gibbs free energies, and Cartesian coordinates (in Å) of all stationary points under study. This material is available free of charge via the Internet at http://pubs.acs.org.

References and Notes

(1) (a) Ward, D. E.; Abaee, M. S. *Org. Lett.* **2000**, *2*, 3937. (b) Ward, D. E.; Souweha, M. S. *Org. Lett.* **2005**, *7*, 3533. (c) Terada, M.; Kouchi, M. *Tetrahedron* **2006**, *62*, 401. (d) Torre, M. F.; Caballero, M. C.; Whiting, A. *Tetrahedron* **1999**, *55*, 8547. (e) Pindur, U.; Lutz, G.; Otto, C. *Chem. Rev.* **1993**, *93*, 741.

(2) Birnary, D. M.; Houk, K. N. *J. Am. Chem. Soc.* **1990**, *112*, 4127.

(3) Yamabe, S.; Dai, T.; Minato, T. *J. Am. Chem. Soc.* **1995**, *117*, 10994.

(4) García, J. I.; Martínez-Merino, V.; Mayoral, J. A.; Salvatella, L. *J. Am. Chem. Soc.* **1998**, *120*, 2415.

(5) Avalos, M.; Babiano, R.; Bravo, J. L.; Cintas, P.; Jiménez, J. L.; Palacios, J. C.; Silva, A. M. *J. Org. Chem.* **2000**, *65*, 6613.

(6) Acevedo, O.; Evanseck, J. D. *Org. Lett.* **2003**, *5*, 649.

(7) Corey, E. J.; Shibata, T.; Lee, T. W. *J. Am. Chem. Soc.* **2002**, *124*, 3808.

(8) (a) Lee, C.; Yang, W.; Parr, R. *Phys. Rev. B* **1988**, *37*, 785. (b) Becke, A. D. *J. Chem. Phys.* **1993**, *98*, 5648. (c) Parr, R. G.; Yang, W. *Density Functional Theory of Atoms and Molecules*; Oxford University Press: Oxford, 1989. (d) Baerends, E. J.; Gritsenko, O. V. *J. Phys. Chem. A* **1997**, *101*, 5383.

(9) Frisch, M. J.; Trucks, G. W.; Schlegel, H. B.; Scuseria, G. E.; Robb, M. A.; Cheeseman, J. R.; Montgomery, J. A., Jr.; Vreven, T.; Pople, J. A.; et al. *Gaussian 03*, revision B. 04; Gaussian, Inc.: Wallingford, CT, 2004.

(10) (a) Tomasi, J.; Persico, M. *Chem. Rev.* **1994**, *94*, 2027. (b) Simkin, B. Y.; Sheikhet, I. *Quantum Chemical and Statistical Theory of Solutions*—A computational Approach; Ellis Horwood: London, 1995; p 78.

(11) (a) Cancès, E.; Mennunci, B.; Tomasi, J. *J. Chem. Phys.* **1997**, *107*, 3032. (b) Cossi, M.; Barone, V.; Cammi, R.; Tomasi, J. *Chem. Phys. Lett.* **1996**, *255*, 327. (c) Barone, V.; Cossi, M.; Tomasi, J. *J. Comput. Chem.* **1998**, *19*, 404.

(12) (a) Thompson, J. D.; Cramer, C. J.; Truhlar, D. G. *J. Chem. Phys.* **2003**, *119*, 1661. (b) Liptak, M. D.; Shields, G. C. *J. Am. Chem. Soc.* **2001**, *123*, 7314. (c) Fu, Y.; Liu, L.; Li, R. Q.; Liu, R.; Guo, Q. X. *J. Am. Chem. Soc.* **2004**, *126*, 814.

(13) Sustmann, R.; Sicking, W. *J. Am. Chem. Soc.* **1996**, *118*, 12562.

(14) Boys, S. B.; Bernardi, F. *Mol. Phys.* **1970**, *19*, 553.

(15) Wong, M. W. *J. Org. Chem.* **2005**, *70*, 5487.